

Novel magnetorheological figuring of KDP crystal

Xiaoqiang Peng (彭小强), Feifei Jiao (焦飞飞)*, Haofeng Chen (陈浩峰),
Guipeng Tie (铁贵鹏), Feng Shi (石峰), and Hao Hu (胡皓)

College of Mechatronics Engineering and Automation, National University of Defense Technology, Changsha 410073, China

*Corresponding author: taurus416@163.com

Received March 22, 2011; accepted April 28, 2011; posted online August 3, 2011

A new process of magnetorheological figuring (MRF) based on the deliquescence theory is proposed to finish KDP crystals. A novel, non-aqueous, and abrasive-free magnetorheological (MR) fluid is explored, and polishing experiments are performed on a self-developed MRF machine. The removal mechanism is reckoned to be the result of a combination of dominant chemical etching and accessorial mechanical drag. The results indicate that the surface roughness of I plate KDP of 80×80 (mm) polished by MRF is 1.2 nm (root mean square (RMS)), and the tool marks are completely removed. The surface accuracy by MRF is 0.035λ (RMS), and the low/middle-frequency errors are significantly corrected after MRF.

OCIS codes: 220.0220, 220.4610, 220.5450.

doi: 10.3788/COL201109.102201.

KDP is a significantly important nonlinear optical crystal. It is widely used in solid state laser systems as frequency converter and electric-optical switch^[1,2]. At present, it is primarily considered as one of the most difficult optical materials to process due to its low hardness, high brittleness, high deliquescence, and extreme sensitivity to temperature changes^[3,4]. Currently, the most common and reasonable process for finishing KDP is single-point diamond turning (SPDT)^[5-7]. America Lawrence Livermore National Laboratory (LLNL) in America and Harbin Institute of Technology (HIT) in China have both developed ultra-precision flatness fly-cutting machines. KDP crystals machined by these equipment have been considerably applied in laser systems.

Due to the increase in improved requirements on energy that laser systems can transmit, demands on laser-induced damage threshold (LIDT) of KDP crystal are accordingly elevated. However, to meet this standard, numerous bottlenecks must be solved immediately. KDP crystals as finished by ultra-precision SPDT, present small scale waviness surface error, which can significantly degrade the LIDT. Research has shown that waviness errors are caused by machine straightness error, vibration, and other ambient factors, and are difficult to correct with the present technology. Thus, methods to eradicate surface waviness errors and achieve fine crystal optics are a key factor to increasing the LIDT that KDP can withstand.

Because of these conditions, researchers began exploring new methods for processing KDP crystals, while continuing to ameliorate machine accuracy and processing parameters. Wang *et al.*^[8] proposed a conventional process which utilized non-aqueous and abrasive-free fluid, and investigated the influence of polishing parameters on material removal and surface quality. Namba *et al.*^[9] put forward an ultra-precision grinding process and researched on the correlation of surface quality with grinding wheels of various diameters. Recently, Menapace *et al.* from LLNL developed a magnetorheological figuring (MRF) process to finish fine KDP optics, and achieved remarkable results of surface roughness of 0.65 nm (root mean square (RMS)), surface accuracy of $\lambda/3$ (PV), and

LIDT of 98.5 J/cm^2 at 1064 nm by 10 ns^[10]. Analysis of current new techniques for polishing KDP reveals that conventional polishing methods lack the ability to finish high-precision KDP surfaces, and that ultra-precision grinding cannot guarantee excellent surface roughness to satisfy practical demands. MRF is a novel technique which can realize high-precision KDP surfaces and improve LIDT on a large scale. At present, domestic MRF research mainly focuses on polishing conventional optical materials, such as K9^[11], SiC^[12], crystallite, etc. Super-smooth surface of sub-nanoscale roughness and highly accurate surface have been achieved. However, an in-depth investigation on deliquescent MRF polishing crystals has not been conducted.

To obtain KDP surfaces of high accuracy and LIDT, we propose a novel process of nonaqueous and abrasive-free MRF based on a deliquescence theory. A kind of nonaqueous and abrasive-free magnetorheological (MR) fluid peculiar to KDP polishing was explored, and experiments were carried out on self-developed polishing apparatus. Surfaces before and after polishing were examined and PSD analysis was conducted to obtain a view of the frequency distribution on the surface.

MRF techniques can realize material removal by controlling the viscosity of the MR fluid, shear yield stress, and its rheological properties under strong and gradual magnetic field. Consequently, the deterministic finish of optical segments with high precision, great efficiency, and little damage can be achieved. The key techniques of MRF require MR fluid, fluid circulating system, and electromagnet that produces a magnetic field in the polishing zone. Currently, commercial or widespread MRF technology mainly focuses on conventional optical parts, such as K9, SiC, etc. Moreover, the MR fluid uses water as the carrier fluid. Due to the water solubility of KDP, the fluid cannot be applied to polish the crystal. In addition, its tendency to fog and damage imposes stringent requirements on the formulation of the MR fluid and the control of its polishing parameters. The newly invented MR fluid should not be or only slightly hygroscopic, nor chemically reactive with KDP. Other considerations include compatibility with experimental

devices and machines, and ease of cleanout.

Considering all the unique material characteristics that KDP crystal possesses, we explored a new kind of non-aqueous and abrasive-free MR fluid. It contains three basic components, namely, organic carrier fluid, spherical carbonyl iron particles with a diameter of $0.5\text{--}2\ \mu\text{m}$ serving as the magnetic particles (Fig. 1), and stabilizer to protect the iron particles from agglomeration and sedimentation. The addition of stabilizer compound will facilitate the formation of a monolayer surrounding iron particles and make the iron particles compatible with the carrier fluid.

To avoid penetration of polishing particles into the KDP surface and the consequent degradation of the LIDT, we excluded abrasive particles from the MR fluid. Instead, a slight amount of deionized water was added to take advantage of the tendency of KDP to deliquescence. The deionized water molecule will act similarly to an oxidant in a chemical-mechanical removal, continuously dissolving KDP surface materials. These materials will be dragged away immediately by the rotating MR ribbon. Finally, material removal will be achieved and a super-smooth surface will be realized. Moreover, long-time exposure to atmosphere will lead to oxidation of iron particles; thus, a PH regulator was appended to adjust the PH value of the fluid to an appropriate range. Based on this new MR fluid, we carried out numerous experiments on a self-developed KDMRF200 machine (Fig. 2).

KDP crystals were rinsed by toluene after MRF polishing. Observation on the KDP surface after cleanout reveals inspiring changes. Figure 3(a) displays the different surface textures before and after polishing. Figure 3(b) shows the surface micro-texture after polishing under magnification of 3000. Flaws and fractures are completely eradicated and there are no fogging points on the surface of the crystal. This proves the feasibility and practicability of the new MR fluid. However, it is necessary to point out that various parameters influence LIDT. Parameters include small-scale waviness, metal particles, fractures, etc.^[12,13]. Although the surface exhibits favorable changes as seen under the microscope after polishing, new defects can be introduced by polishing. To explore this situation, a laser transmittance test is necessary to compare the surfaces before and after polishing. Due to equipment limitation, the test could not be conducted. This will be the focus of our next research.

The removal mechanism for conventional optical MRF

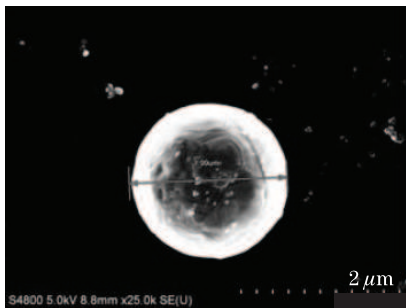


Fig. 1. Microscopic view of iron particles under SEM.

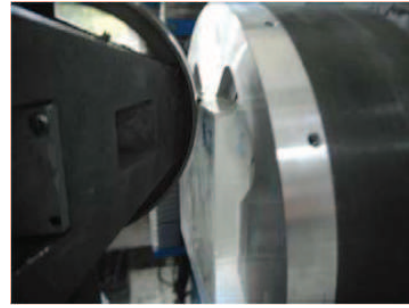


Fig. 2. Photograph of MRF polishing KDP.



Fig. 3. KDP surface appearances after polishing. (a) Comparison of surface before and after MRF and (b) KDP surface micro-shape after MRF.

polishing includes mechanical effects, chemical effects, and surface flowing effects. Mechanical effects are the most dominant^[14]. Figure 4(a) schematically depicts the removal model of conventional MRF polishing materials. There is a gap of approximately $100\text{--}150\ \mu\text{m}$ between the magnetic core and the optical surface^[15,16]. The combination of drag force F_d and normal force F_n exerted on each polishing particle produces a pressure large enough to allow the particle to penetrate a certain depth into the material. This is shown in Fig. 4(b). Along with the rotation of the stiffened MR fluid ribbon, the abrasive particle moves at a certain speed of v against the optic and introduces shear stress, under which, material removal is realized.

Compared with the dominant mechanical removal in a conventional material MRF polishing, the novel process for KDP polishing utilizes its tendency to deliquescence. By adding a small portion of deionized water, the surface material will dissolve upon contact with water, and the rotating ribbon will remove the dissolved material from the substrate, as illustrated in Fig. 5. The water molecule that has not entered the polishing zone is surrounded by a monolayer formed by the carrier fluid molecules through chemical bonding. Upon entering the polishing zone, pressure acting on the water molecule can break the chemical bonding. Consequently, the water molecule will make contact with the KDP surface directly and realize material dissolution and removal. It is necessary to point out that the protecting monolayer formed through chemical bonding will not break when it is in its freeform state, which explains why carrier fluid residues on the KDP surface will not lead to contamination and fogging.

To validate our deduction further, spot-taking experiments were performed to calculate the remove function and analyze its unique properties from normal MRF

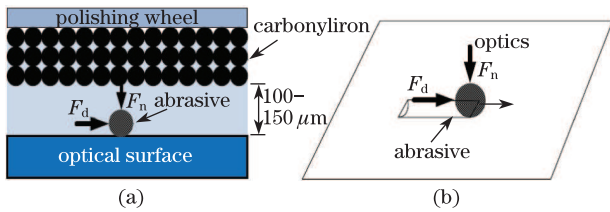


Fig. 4. Schematic of MRF polishing conventional optical materials.

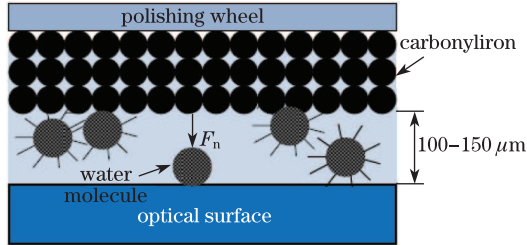


Fig. 5. Schematic of KDP material removal by MRF.

spots. First, MR fluid with 0 wt.-% of deionized water was utilized to take a remove spot by employing the parameters in Table 1 with penetration of 0.1 mm and duration of 1 min. Figure 6(a) exhibits the result in a Zygo file. The peak remove rate (PRR) is only $0.044 \mu\text{m}/\text{min}$, and the volume remove rate (VRR) is $1.13 \times 10^5 \mu\text{m}^3/\text{min}$. Subsequently, 2.5 wt.-% of deionized water was added to the fluid. After a 4 s duration, spots taken under this setting, as shown in Fig. 6(b), demonstrate huge disparity. The PRR is $5.63 \mu\text{m}/\text{min}$, and the VRR is $1.74 \times 10^7 \mu\text{m}^3/\text{min}$, more than 150 times than those of Fig. 6(a). Compared with material dissolution in water, material removal achieved by mechanical function can be completely ignored. This strongly supports our deduction that dissolution is mainly responsible for the material removal in the new process.

During the conduct of the other experiments, an interesting phenomenon is discovered. Figure 7 displays four spots. The two horizontal spots were taken with a penetration of 0.1 mm, and the two vertical spots were taken at 0.2 mm penetration. Other parameters were the same. The PRRs of the four remove functions are all within $1.73 \pm 2\% \mu\text{m}/\text{min}$. This discovery indicates that PRR has no binding relations with penetration. In other words, the mechanical removal under various penetrations has minimal influence on PRR. Obtaining the same PRR could only be explained by material dissolution, which will not change with different levels of penetration. Further investigation, to fully understand the removal mechanism, is ongoing.

In the removal process, another point of interest involves identifying the carbonyl participation of iron particles in the material removal and embedment into KDP, which can significantly degrade the KDP LIDT performance. Observations were made on surface texture and detections of surface chemical elements were performed on the polished surface. Figure 8(a) represents the comparison between the polished surfaces before and after rinsing. Several residual carbonyl iron particles are visible on the rinsed surface. To eliminate the residual particles, a cleanout procedure was developed. The optic was immersed in the cleanout fluid, accompanied

with rotation or movement to sufficiently remove the residues, and placed in a drying cabinet. Subsequently, the workpiece was observed under the microscope, as demonstrated in Fig. 8(b). The attached impurities have completely cleared up. Importantly, this procedure does not import surface fogging points.

To further explore the likelihood of embedment of the carbonyl iron particles into the KDP material, a spectrometer was adopted to mensurate the crystal surface chemical ingredients on discrete areas. A total of 20 areas measuring $15 \times 15 (\mu\text{m})$ were spotted, and the results exhibited considerable similarity. Figure 9 demonstrates one of the spectrometric maps of the surface chemical composition. Table 2 lists the percentages of different elements.

As shown in Fig. 9 and Table 2, four chemical elements, namely, P, O, K, and C, are detected. We believe they are the chemical ingredients of KDP and rinse fluid. Fe is not detected, which may be due mainly to the following reasons: (1) under the influence of a strong magnetic field, the majority of carbonyl iron is tightly attached to the bottom of the fluid ribbon, hence, only a few particles exist on the ribbon top and contact with the KDP crystal; (2) these dissociative spherical iron particles with a diameter of $0.5\text{--}2 \mu\text{m}$ are surrounded by

Table 1. Settings of KDMRF200

Wheel Diameter (D/mm)	Magnet Electricity (I/A)	Wheel Speed (n/r·min ⁻¹)
100	4.0	180
Flux (Q/L/h)	Penetration (d/ μm)	Viscosity ($\eta/\text{Pa}\cdot\text{s}$)
45	150	1.5

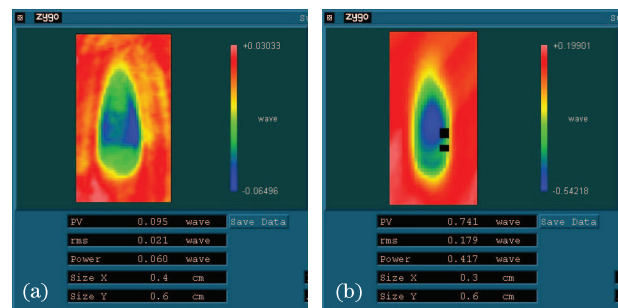


Fig. 6. Spots taken under different percentages of water. (a) 0 and (b) 2.5 wt.-% water.

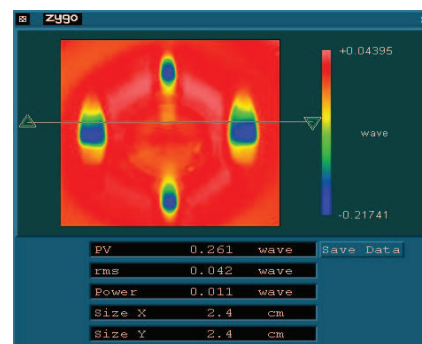


Fig. 7. Spots at different penetrations.

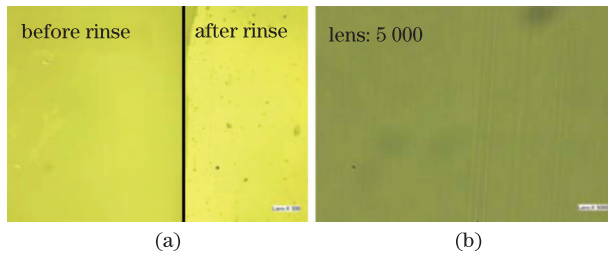


Fig. 8. KDP polished surfaces before and after rinsing.

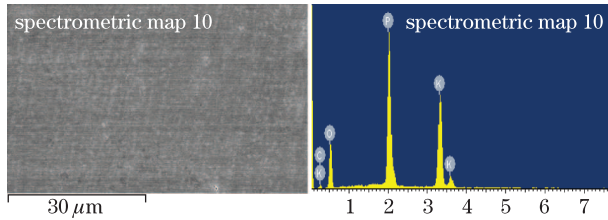


Fig. 9. Spectrometric map of surface chemical compositions of KDP surface.

a monolayer compatible with the carrier fluid. Particles would slide or roll on the KDP surface and will not penetrate into the crystal surface. Their tracks are observable under a magnification of 5000, as shown in Fig. 6(b). This convincingly confirms our deduction.

To thoroughly examine the KDP surface quality after polishing, numerous experiments were performed on a self-developed KDMRF-200 apparatus. The operational settings, which are listed in Table 1, were kept constant in all experiments.

The 80×80 (mm) KDP crystals provided by Shandong University, categorized as I class, served as frequency doubler in solid laser systems. The polishing adhered to the procedure of a previous study^[11]. The polishing and taking the remove function were both finished by SPDT prior to the conduct, taking into consideration that surface accuracy achieved by SPDT should be below 1λ ($\lambda = 632.8$ nm), and there should be no areas of fracture and breakpoints because of material brittleness.

Surface roughnesses, before and after the MRF, were measured with a Zygo NewView 700 white-light interferometer. The spot areas were taken with a $50\times$ lens (Fig. 10).

In Fig. 8, surface roughness by SPDT is 2.3 nm (RMS) and 1.8 nm (Ra). It significantly improved to 1.2 nm (RMS) and 0.9 nm (Ra) after the MRF adopting parameters in Table 1. To probe the ability of the new process to remove tool marks, we drew a selected line along the tool feeding direction in Fig. 10(a) and a random line in Fig. 10(b). PSD analysis was conducted (Fig. 11).

The solid curve represents the PSD result of SPDT, whereas the dotted one indicates that of MRF. Clearly, PSD distribution achieved significant melioration. The sharp step marked by the ellipse, which we deduced to be the result of the tool feeding step of approximately $2 \mu\text{m}/r$, has been completely eliminated by MRF. This result provides credible evidence for the capacity of the new process to remove tool marks.

Surface accuracy was also measured with a Zygo GPI 1000 interferometer before and after MRF polishing. Figure 12(a) represents the KDP crystal surface error

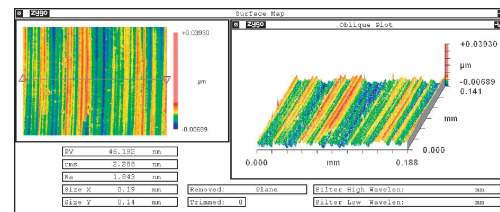
($PV = 1.377\lambda$; $RMS = 0.234\lambda$) after SPDT and before MRF. After two iterations by MRF, the surface accuracy improved to $PV = 0.257\lambda$, $RMS = 0.035\lambda$, as shown in Fig. 12(b). Moreover, after conducting the spectrum analysis, the PSD curve lines in Fig. 13 show evident improvement with a scope of low/middle frequency errors caused by SPDT. However, as a sub-aperture machining process, MRF can easily introduce high-frequency errors. This tendency is evident in Fig. 13.

Because of equipment limitation, we did not perform LIDT experiments on polished KDP crystals. This should be carried out in future work.

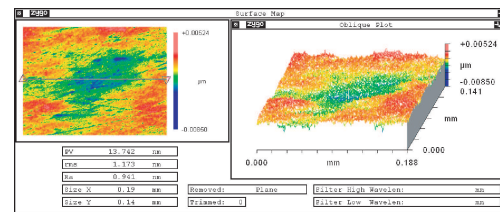
In conclusion, domestic laboratories focus mainly on finishing KDP by SPDT, and minimal research has been implemented on the MRF process. Thus, we deem this responsibility as our own and perform an innovative endeavor, with the support of our laboratory. After research and experiments, we find a novel method to polish KDP crystals by MRF and successfully improve part of an 80×80 (mm) KDP from a surface accuracy of

Table 2. Percentage Distribution of Chemical Composition

Elements	Weight	Atom
C	5.47	10.33
O	36.36	51.59
P	28.21	20.67
K	29.97	17.40



(a)



(b)

Fig. 10. KDP surface roughnesses before and after MRF.

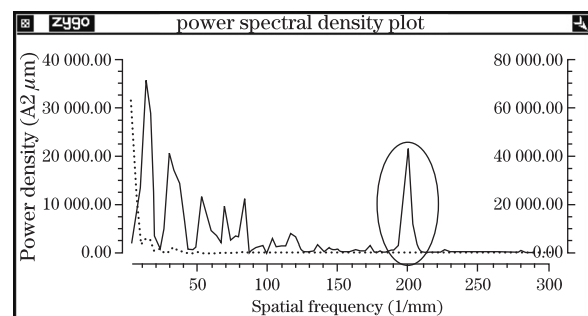


Fig. 11. PSD analysis.

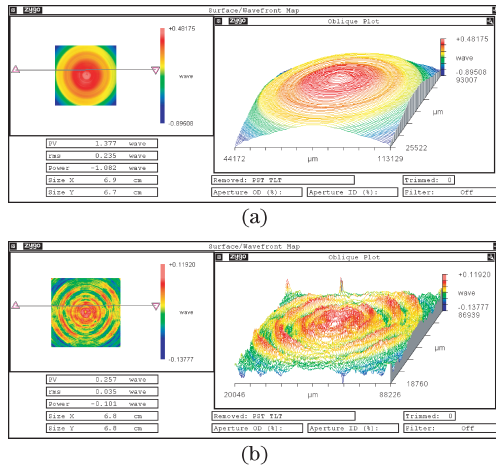


Fig. 12. Surface errors before and after MRF. (a) by SPDT [1.377λ (PV), 0.234λ (Rms)] and (b) by MRF [0.257λ (PV), 0.035λ (Rms)].

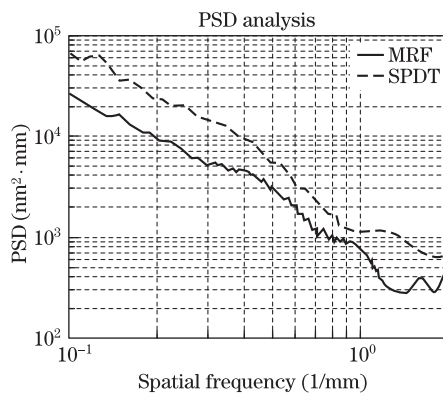


Fig. 13. PSD comparison before and after MRF.

PV = 1.377λ to 0.257λ . Based on this, we present several conclusions and directions.

(1) Considering the existing problems in the conventional machining process and the uniqueness of KDP materials, we propose a novel nonaqueous and abrasive-free MRF process based on a deliquescence theory. The proposed method has been shown to achieve super-smooth KDP surface.

(2) A new nonaqueous and abrasive-free MR fluid is developed. All the components are properly selected. The new MR fluid, which facilitates cleanout, shows compatibility with the experimental devices and machines. Importantly, this water-containing MR fluid does not cause fogging problems due to its peculiar dissolution theory.

(3) The removal mechanism in MRF polishing must be sufficiently understood. We infer that material removal

can be realized through a combination of material dissolution in water and the high speed rotation of the ribbon, which can immediately drag away the dissolved material. Simultaneously, carbonyl iron particles dissociate on the top of the rotating ribbon and slide and roll on the KDP surface. This prevents embedment into KDP material.

(4) An analysis of the surface quality before and after MRF polishing reveals that roughness achieved by MRF can reach 1.2 nm (RMS), and that the method can totally eliminate tool marks imported by SPDT. Additionally, after two iterations, the surface accuracy is improved to 0.035λ (RMS) and performances on low/middle frequency errors are significantly ameliorated. However, high-frequency errors are imported by MRF. This can be solved through algorithm and path optimization which should be investigated in future studies.

This work was supported by the National Natural Science Foundation of China under Grant Nos. 50775217 and 50875256.

References

1. F. Yang, *Opt. Tech.* (in Chinese) **29**, 649 (2003).
2. V. I. Salo, V. F. Tkachenko, M. A. Rom, V. M. Puzikov, and M. I. Kolybayeva, *Proc. SPIE* **3359**, 540 (1998).
3. H. Wang, J. Wang, T. Sun, and L. Zhang, *Acta Armentarii* (in Chinese) **27**, 911 (2006).
4. I. M. Thomas, M. R. Kozlowski, G. Edwards, K. Stanion, and B. Fuchs, *Proc. SPIE* **1642**, 137 (1991).
5. B. A. Fuchs, P. P. Hed, and P. C. Baker, *Appl. Opt.* **25**, 1733 (1986).
6. S. Dong, X. Zhang, and J. Wang, *Tool Technol.* (in Chinese) **39**, 19 (2005).
7. Y. Namba, K. Yoshida, H. Yoshida, and S. Nakai, *Proc. SPIE* **3266**, 320 (1998).
8. B. Wang, H. Gao, X. Teng, and R. Kang, *J. Synth. Cryst.* (in Chinese) **39**, 29 (2010).
9. Y. Namba, K. Yoshida, H. Yoshida, and S. Nakai, *Proc. SPIE* **3244**, 320 (1998).
10. J. A. Menapace, P. R. Ehrmann, and R. C. Bickel, *Proc. SPIE* **7504**, 750414 (2009).
11. F. Shi, Y. Dai, X. Peng, and C. Song, *Opt. Precis. Eng.* (in Chinese) **17**, 1859 (2009).
12. X. Li, X. Liu, Y. Zhao, J. Shao, and Z. Fan, *Chin. Opt. Lett.* **8**, 598 (2010).
13. X. Li, Y. Zhao, X. Liu, J. Shao, and Z. Fan, *Chin. Opt. Lett.* **8**, 615 (2010).
14. F. Shi, Y. Dai, X. Peng, N. Kang, and Z. Liu, *J. National Univ. Defense Technol.* (in Chinese) **31**, 25 (2009).
15. A. Shorey, W. Kordonski, and M. Tricard, *Proc. SPIE* **5533**, 99 (2004).
16. A. B. Shorey, "Mechanisms of material removal in magnetorheological finishing (MRF) of glass" PhD. Thesis (University of Rochester, Rochester, 2000).